Oscillation-induced sand dunes in a liquid-filled rotating cylinder

Veronika Dyakova*
Laboratory of Vibrational Hydromechanics, Perm State Humanitarian Pedagogical University and Perm National Research Polytechnic University, Perm, Russia

Victor Kozlov† and Denis Polezhaev‡
Laboratory of Vibrational Hydromechanics, Perm State Humanitarian Pedagogical University, Perm, Russia
(Received 11 July 2016; revised manuscript received 10 October 2016; published 19 December 2016)

The dynamics of granular medium in a liquid-filled horizontal cylinder with a time-varying rotation rate is experimentally studied. When the cylinder is purely rotated, the granular medium develops an annular layer near the cylindrical wall. The interface between fluid and sand is smooth and axisymmetric. The time variation of the rotation rate initiates the azimuthal oscillation of the liquid in the cylinder's frame of reference and provokes the onset of quasisteady relief in the form of regular dunes. The stability of the axisymmetric sand surface and dynamics of regular dunes are examined. It is found that the ripple formation is provoked by the quasisteady instability of the Stokes boundary layer. In the range of high Reynolds numbers, the ripple formation occurs at a constant critical Shields number $\theta_c \simeq 0.05$. The spatial period of the relief is not sensitive to the fluid viscosity and granule diameter; it is determined by the amplitude of oscillation and ratio between the oscillation frequency and mean rotation rate. Long-term experiments show that there are forward and backward azimuthal drifts of dunes. An initial analysis of the issues related to the dune migration is provided.

DOI: 10.1103/PhysRevE.94.063109

I. INTRODUCTION

It is known that surface waves in nearshore waters induce to-and-fro motion near the seabed. This motion interacts with the seabed, modifies its geometry, and generates bed forms, which are known as ripples. Stokes [1] showed that in a surface wave, in addition to the oscillatory motion, fluid has a steady second-order drift in the direction of wave propagation. The presence of a unidirectional component of water flow is clearly relevant to questions that involve the ripple migration initiated by water waves [2,3]. The migration of subaqueous sand patterns is an important component of coastal sediment dynamics (see, e.g., [4]). The seabed geometry directly affects fluid motion and controls sediment transport in coastal and continental shelf areas.

Under the to-and-fro motion of liquid, individual grains begin to roll over the flat bed and form small ridges, which are called rolling-grain ripples [5]. Rolling-grain ripples are transient and evolve into larger vortex ripples: the flow over the ripples generates vortices that transport sand from the ripple troughs and bring it towards the ripple crest (see, e.g., [6]). For a sufficiently large liquid velocity, the transition to a sheet flow occurs, and the ripples are washed out from the sand bed, which becomes flat again (see, e.g., [7]). Sheet flow with a high sediment concentration causes notably large sediment transport rates.

Despite the practical relevance of understanding the bed morphology and related phenomena and the great interest of many authors, important questions remain unanswered: What are the relevant dynamical mechanisms that control ripple formation? What determines the time scales and length scales of ripples? In a review [8], these questions and related problems were discussed for the case of ripples under unidirectional flow conditions.

This paper concentrates on the ripple formation and spatiotemporal evolution of ripples under oscillatory liquid flow. Ripple formation under oscillatory flow has been extensively investigated under laboratory conditions [3,7,9–16]. In the experiments, oscillatory flow is generated in a wave tunnel [9], a stationary tank using water surface waves [3,7,10,11], an oscillating container [12–15], or a rapidly rotating drum using water surface waves [16]. A distinctive feature of the latter study is the presence of rotation: Dyakova *et al.* [16] considered that in the frame of reference of a horizontal rotating cylinder, the gravitational force oscillates and produces fluid oscillation in an annular liquid layer.

This paper extends the study of Dyakova *et al.* [16] to the case of a completely liquid-filled cylinder with a time-varying rotation rate:

$$\Omega = \Omega_r + \varphi_0 \Omega_{\rm osc} \sin \Omega_{\rm osc} t, \tag{1}$$

where Ω_r is the mean rotation rate, φ_0 is the angular amplitude of azimuthal oscillation, and $\Omega_{\rm osc}$ is the radian frequency of oscillation.

In a purely rotating cylinder, the granular medium is uniformly distributed near the cylindrical wall: The interface between liquid and sand is axisymmetric. If the rotation rate is time varying, liquid oscillates in the cylinder's frame of reference and provokes sand bed instability.

The dynamics of the liquid inside a cylinder with a time-varying rotation rate is qualitatively similar to libration-driven liquid flows. Better knowledge of these flows is of great interest in astrophysics, where libration is driven by gravitational interactions and used to investigate the interior structure of planets [17–20].

In this paper, we present an experimental method to demonstrate sand bed instability under time-varying rotation

*dyakova@pspu.ru
†kozlov@pspu.ru
‡polezhaev@pspu.ru

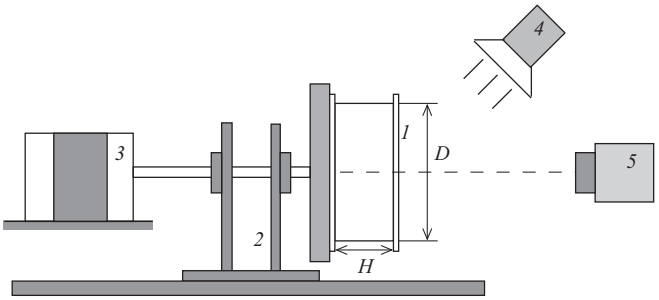

FIG. 1. Scheme of the experimental setup.

and report experimental results for the length scale of sand ripples and their long-term evolution.

The outline of this paper is as follows: the experimental setup is described in Sec. II. The experimental results for the stability of an axisymmetric sand bed and time evolution of ripples and a discussion of the length scale of the dunes are presented in Sec. III. The conclusions are provided in Sec. IV.

II. EXPERIMENTAL SETUP

The scheme of the experimental setup is shown in Fig. 1. It consists of a hollow transparent cylinder with an inner radius $R = D/2 = 6.3$ or 7.2 cm and length $H = 7.8$ or 2.2 cm. The cylinder was filled with a water-glycerol solution (kinematic viscosity $\nu = 3.8$–13 cSt, density $\rho_l = 1.12$–1.17 g/cm^3) and seeded with glass spheres of density $\rho_s = 2.50$ g/cm^3 $\pm$ 2%. Experiments were performed with particles of two different mean diameters: $d = 0.018$ cm $\pm$15% or 0.009 cm $\pm$10%. The mass of the granular medium was 80 g in the cylinder of radius $R = 7.2$ cm and 200 g in the cylinder of radius $R = 6.3$ cm.

Cylinder *1* was supported by roller bearings *2* and mounted on a massive horizontal platform. Stepper motor *3* was coupled to the cylinder and provided rotation about its horizontal axis with a mean angular velocity Ω_r up to 75 rad/s and accuracy of 0.05%. The stepper motor also provided harmonic oscillation of the angular velocity in the form of $\varphi_0\Omega_{\rm osc}\sin\Omega_{\rm osc}t$, where $\Omega_{\rm osc}$ could be selected between 2 and 75 s^{-1} and accuracy of 0.05%. In terms of dimensionless numbers, we explored the following ranges: the ratio between the oscillation frequency and mean rotation rate $f \equiv \Omega_{\rm osc}/\Omega_r \in [0.03; 1]$ and parameter $\epsilon \equiv \varphi_0 f \in [0; 0.5]$.

Each experiment followed a standard protocol. The cylinder was slowly accelerated from rest to several revolutions per second. After a solid body rotation was reached, the granular medium developed an annular layer near the cylindrical wall. The thickness of the axisymmetric annular layer was $h_0 = 0.56$ cm in the cylinder of radius $R = 7.2$ cm and 0.45 cm in the cylinder of radius $R = 6.3$ cm. Then, the stepper motor was activated to oscillate at definite frequency $\Omega_{\rm osc}$ and parameter ϵ. To determine the threshold of ripple formation, we followed the interface between the fluid and granular medium in stroboscopic illumination, which was emitted by lamp *4*. Each experiment lasted for dozens of minutes ($\sim 10^4$–10^5 cycles of oscillation).

If the surface remained axisymmetric for a sufficiently long time, we terminated the experiment and began a new one at a larger value of ϵ. As soon as the axisymmetric sand surface became disturbed, photo registration by the DSLR camera *5* Nikon D7000 and lenses Nikkor 50 mm f/1.8 G was initiated.

The main scope of this paper is to determine the stability criterion for the axisymmetric surface of the granular medium, the length scale of regular ripples, and a physical explanation of the ripple formation and related issues.

III. EXPERIMENTAL RESULTS

A. Stability of an axisymmetric sand bed

When the horizontal cylinder was stationary, the granular medium was at rest at the bottom of the cylinder. When the cylinder was rotated with a low to moderate angular velocity, its rising side dragged spherical particles from the bottom. After a few revolutions, an almost uniform suspension of glass spheres originated in the rotating low-viscosity fluid. In a rapidly rotating cylinder, the annular granular layer developed [Fig. 2(a)]. Without cylinder oscillation, the fluid and granular medium underwent a solid-body rotation, and the interfacial surface was axisymmetric.

In the experiments, we provided rapid rotation, when the ratio of the gravitational force to the centrifugal force was

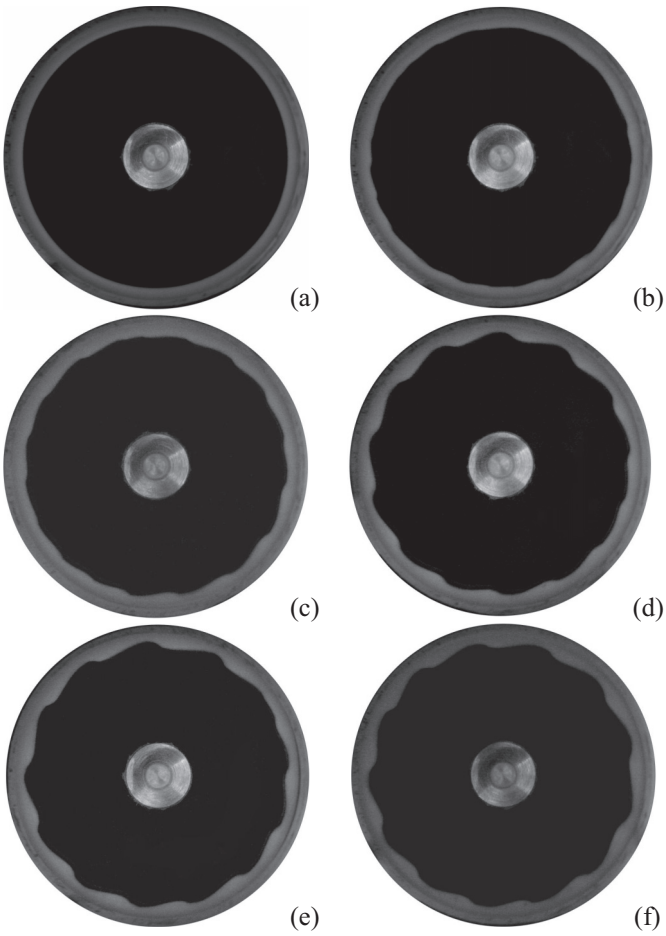

FIG. 2. Time evolution of dunes: $R = 7.2$ cm, $h_0 = 0.56$ cm, $\nu = 5.0$ cSt, $d = 0.018$ cm, $\Omega_r = 31.4$ rad/s, $\Omega_{\rm osc} = 6.28$ s^{-1}, $\epsilon = 0.15$ (threshold value of ϵ is 0.135). Images (a)–(f) were captured at time $t = 0$, 5, 15, 30, 45, and 55 min. The rotation is counterclockwise.

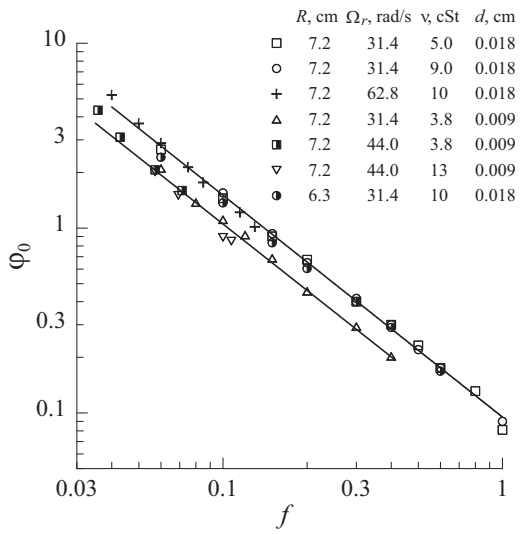

FIG. 3. Angular amplitude of oscillation versus the nondimensional frequency of oscillation at the threshold of ripple formation. The solid lines correspond to the best data fit for two types of glass particles: $\varphi_0 \sim f^{-1.2}$.

$\Gamma = g/\Omega_r^2 a \sim 0.1$ (a is the radius of the axisymmetric sand bed), which is equivalent to a weak effect of gravitational force.

The time variation of the rotation rate initiated the azimuthal oscillation of fluid in the cylinder's frame of reference, whose frequency and amplitude were determined by $\Omega_{\rm osc}$ and ϵ. In the experiments with fixed Ω_r and $\Omega_{\rm osc}$ and increasing ϵ, the initially axisymmetric interface between the fluid and granular medium became unstable due to the ripple growth. When the angular amplitude of oscillation φ_0 increased, we observed two regimes of ripple formation: rolling-grain ripples with grains moving back and forth at the interface between the granular medium and fluid and quasisteady dunes with perpendicular crests to the fluid oscillation [Figs. 2(b)–2(f)].

At the threshold of ripple formation, irregular dunes of small height were observed. At larger values of ϵ, the ripples became regular and covered the entire surface area of the granular medium. The typical evolution of an initially axisymmetric sand bed, which destabilized under the action of an oscillatory flow, is shown in Fig. 2. Typically, ripples have an asymmetrical cross section: one slope is steep and the other is gentle.

The experimental data on the threshold of ripple formation are presented in the plane of the angular amplitude of oscillation $\varphi_0 \equiv b/a$ (b is the amplitude of liquid oscillation; a is the radius of axisymmetric sand bed) and nondimensional frequency of oscillation $f \equiv \Omega_{\rm osc}/\Omega_r$ (Fig. 3). The rotation rate and frequency of oscillation were varied to cover various ranges of f and φ_0. According to the data in Fig. 3, the critical value of the amplitude of oscillation strongly depends on the particle diameter and is affected by the liquid viscosity (e.g., compare two types of triangles): a greater viscosity corresponds to a smaller amplitude at the threshold of ripple formation. The solid lines correspond to the law: $\varphi_0 \sim f^{-1.2}$.

In a recent study by Rousseaux *et al.* [14], the stability of the horizontal sand-fluid interface in a vertical cylindrical container with rotary oscillation was studied. Similar to the problem discussed here, they separated two different thresholds: one for grain movement and the other for ripple formation. In other words, ripple formation requires the initiation of grain motion. In our experiments, the threshold for the grain motion is difficult to precisely determine, and we were concerned with the threshold for ripple formation.

We selected the Shields number θ as a control parameter for this instability, which is the ratio between the viscous shear stress at the top of the sand bed and the apparent weight of a single particle. The critical Shields number is required to initiate the motion of the sand particles and associated dune growth. According to [21], the typical critical Shields number is $\theta_c \simeq 0.05$.

We can estimate θ_c by defining the viscous shear stress and apparent weight as

$$\nu\rho_l b\Omega_{\rm osc} d^2/\delta \tag{2}$$

and

$$(\rho_s - \rho_l)\Omega_r^2 a d^3, \tag{3}$$

respectively. Here, b is the amplitude of liquid oscillation; $\delta = \sqrt{2\nu/\Omega_{\rm osc}}$ is the thickness of the Stokes boundary layer near the sand surface because of the liquid oscillation. The rapid rotation of the cylinder implies a specific definition of the apparent weight: We consider the inertial centrifugal force instead of the gravitational force [Eq. (3)].

Finally,

$$\theta = \frac{\nu b\Omega_{\rm osc}}{(\rho - 1)\Omega_r^2 a d\delta}, \tag{4}$$

where $\rho = \frac{\rho_s}{\rho_l}$ is the relative density of granules with respect to the liquid.

The experimental verification of $\theta_c \simeq 0.05$ is challenging because the flow in the Stokes layer is laminar only in a limited range of Reynolds numbers. A popular assumption to treat the stability of time-dependent states is the quasisteadiness: the basic flow is assumed to vary so slowly in comparison with the growth of a disturbance that it can be treated as a steady basic state using an instantaneous, frozen profile. Thus, according to the quasisteady theory [22], the crisis of the oscillatory motion of a liquid confined between parallel plates, when one plate is at rest and the other oscillates, is determined by the stability of the velocity profile in the phase of zero flow rate. The analysis finds that for $\mathrm{Re}_\delta > 10^2$, the oscillatory flow is unstable to perturbations with a nondimensional wave number, which is scaled with the thickness of the Stokes boundary layer: $k_\delta = 0.5$. Reynolds number Re_δ is defined with the boundary layer thickness according to

$$\mathrm{Re}_\delta = \frac{b\Omega_{\rm osc}\delta}{\nu}. \tag{5}$$

A similar effect was found for the stability problem of the Stokes layer in a stationary planar channel [23] and a horizontal rotating cylinder that was partially filled with liquid [24]. In both cases, the intensive vortices rise in a certain phase of the cycle and vanish in the remainder of the cycle. In addition, the experimental data analysis of Kozlov and Polezhaev [24] reveals that the wave number of vortices, which is defined with the boundary layer thickness, is $k_\delta \approx 0.5$.

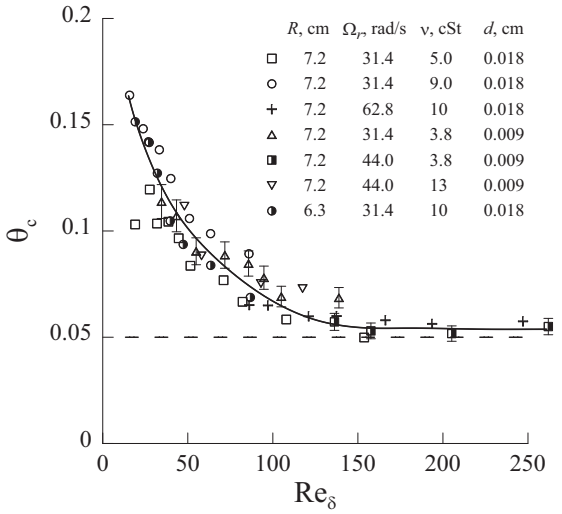

FIG. 4. Critical Shields number for the onset of bed form instability as a function of the Reynolds number. The dotted line corresponds to the critical Shields number $\theta_c = 0.05$. Here and below (if not stated otherwise), the solid line is a guide for the eye.

We measured the wavelength λ at the initial phase of the ripple growth and calculated the wave number $k_\delta \equiv 2\pi\delta/\lambda$. The experimental results are consistent with the obtained data in the quasisteady theory: $k_\delta = 0.56 \pm 0.10$. Figure 4 demonstrates the experimental results of the threshold of ripple formation in the plane of Re_δ and θ_c. In the range of large Reynolds numbers ($\mathrm{Re}_\delta > 100$), the experimental data on the critical Shields number are consistent with the typical value $\theta_c \simeq 0.05$ [21]. With the data on the initial wave number k_δ, the curve kink at approximately $\mathrm{Re}_\delta = 100$ in Fig. 4 verifies that ripple growth is provoked by the onset of quasisteady instability of the oscillatory fluid flow.

This result is consistent with the experimental observations of Rousseaux *et al.* [13]. Rousseaux *et al.* studied subaqueous sand ripples in an oscillating annular cell and revealed that the critical Shields number θ_c tended to a constant value in the range of $\mathrm{Re}_\delta > 100$. Rousseaux *et al.* also measured the wavelength of sand ripples before the coarsening process became important (see Fig. 7 in [13]). Based on these measurements, we found that the wave number k_δ varied in the range of 0.4–1.0 for the fine grains $\delta/d \gg 1$. This phenomenon was not explained in [13], but we believe that the exactly quasisteady instability of the oscillatory flow is responsible for ripple formation.

B. Time evolution and length scale of ripples

Regular relief develops over a long period of time: depending on the experimental conditions, ripples continue to grow for a few minutes or dozens of minutes. Figure 5 shows the dependence of the relative height h/h_0 and azimuthal length λ/h_0 of the dunes on time. Here, h is the distance from the cylindrical wall to the crest and the toe of dunes, h_0 is the thickness of the axisymmetric annular layer of granular medium, and λ is the distance between crests of adjacent dunes. The empty circles in Fig. 5(a) correspond to the crest height; the filled circles correspond to the thickness at the toe

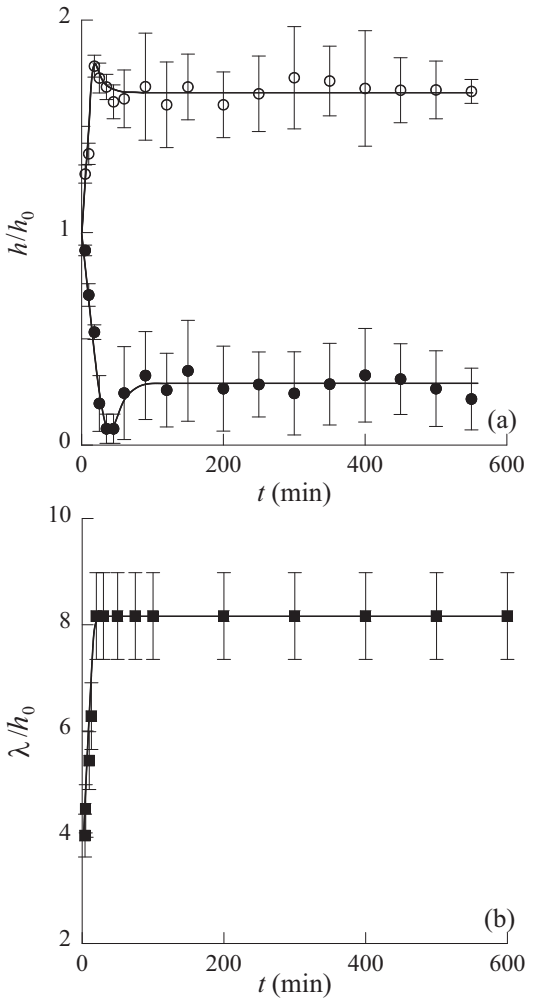

FIG. 5. Dependence of the relative height h/h_0 (a) and azimuthal length λ/h_0 (b) of dunes on time: $R = 6.3$ cm, $h_0 = 0.45$ cm, $\nu = 10$ cSt, $d = 0.018$ cm, $\Omega_r = 31.4$ rad/s, $\Omega_{\mathrm{osc}} = 12.6\ \mathrm{s}^{-1}$, $\epsilon = 0.163$. (a) The empty and filled circles were obtained for the thickness at the crest and toe of the dunes.

of the dunes. In the growth phase of the ripple formation, the dunes grew because of the sand transport from toe to crest. Comparing the data in Figs. 5(a) and 5(b), we conclude that after approximately half an hour, the quasisteady state was reached: the spatial period and height of the relief remained constant.

In the experiments, we used stroboscopic illumination to visually determine the threshold of ripple formation. The threshold can also be determined from the dependence of the dimensionless azimuthal length λ/h_0 on parameter ϵ: the azimuthal length linearly increases with ϵ (Fig. 6).

Specific features appeared at high values of ϵ: in a certain phase of fluid oscillation, surface granules began floating, and the dune slopes became gentler [e.g., comparing Figs. 7(a) and 7(f)] and the sheet flow occurred. Furthermore, the height of the dunes decreased and the azimuthal size remained constant (Figs. 6 and 7 at $\epsilon > 0.4$).

Figure 8 shows the dependence of the dune wavelength on the amplitude of oscillation. The experiments were performed at a fixed rotation rate $\Omega_r = 31.4$ rad/s and various frequencies

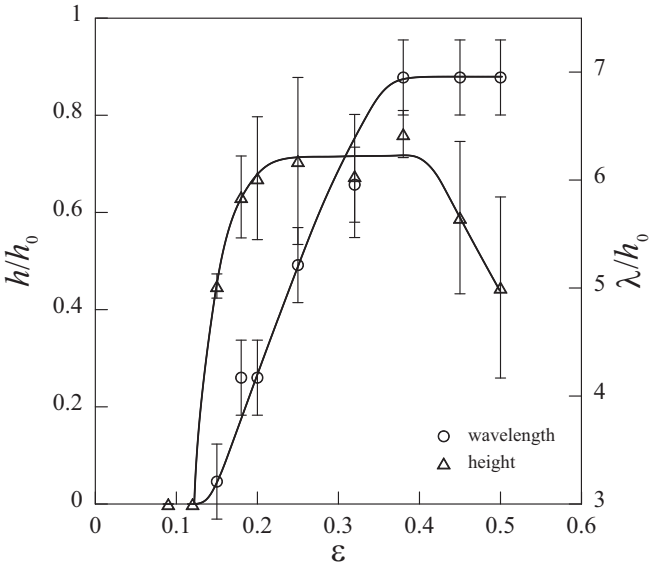

FIG. 6. Dependence of the relative maximum height and spatial period of dunes on ϵ: $R = 7.2$ cm, $h_0 = 0.56$ cm, $\nu = 5.0$ cSt, $d = 0.018$ cm, $\Omega_r = 31.4$ rad/s, $\Omega_{\rm osc} = 6.28$ s^{-1}.

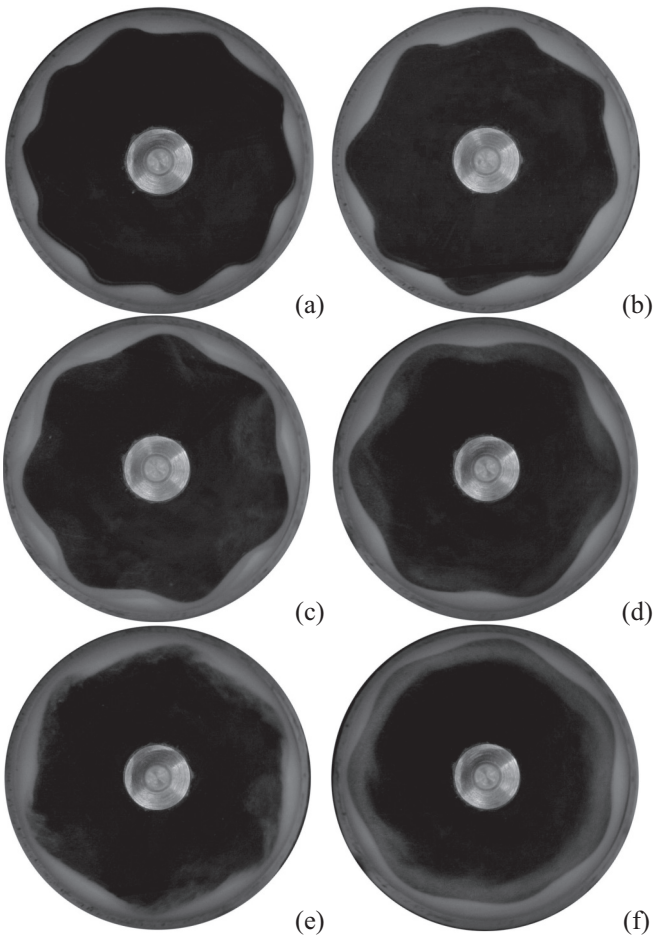

FIG. 7. Regular dunes in a rotating and oscillating cylinder: $R = 7.2$ cm, $h_0 = 0.56$ cm, $\nu = 5.0$ cSt, $d = 0.018$ cm, $\Omega_r = 31.4$ rad/s, $\Omega_{\rm osc} = 6.28$ s^{-1}, $\epsilon = 0.18$, 0.25, 0.32, 0.38, 0.45, and 0.50 [(a)–(f)]. The rotation is counterclockwise.

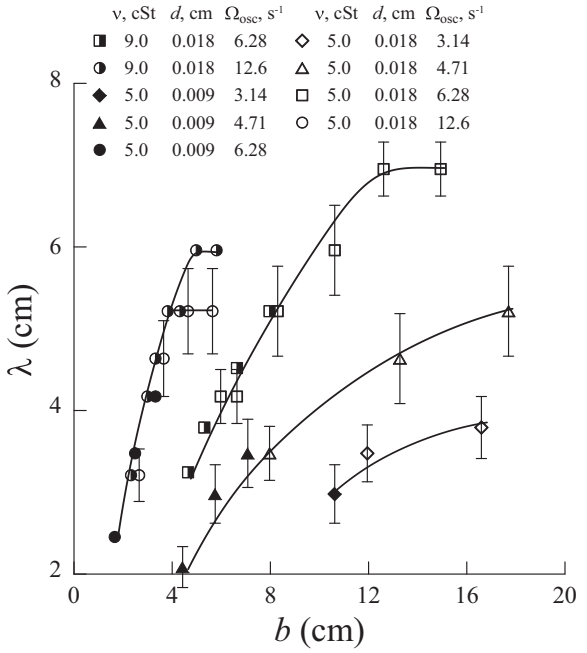

FIG. 8. Dependence of the spatial period of quasisteady relief λ on the amplitude b of the cylinder oscillation: $R = 7.2$ cm, $\Omega_r = 31.4$ rad/s.

of oscillation $\Omega_{\rm osc}$. The open, semifilled and filled symbols of the same type (squares, circles, triangles, and diamonds) illustrate the data that were obtained at identical values of $\Omega_{\rm osc}$ or $f \equiv \Omega_{\rm osc}/\Omega_r$. The data obtained in the experiments with granules of two sizes and liquids of different viscosities are consistent with one another for equal f. This result indicates that nondimensional frequency f is one of the governing parameters of the problem.

The starting point for discussion of the ripple length variation is the experimental fact that the ripple length of sand ripples is proportional to the liquid amplitude: λ/b is constant. This relation was first noted by [25] and later verified by [12,14,15]. However, as shown in Fig. 8, the ripple size does not linearly depend on the amplitude of oscillation. The data in Fig. 8 clearly show that the ripple length depends on both the amplitude of oscillation b and ratio $\Omega_{\rm osc}/\Omega_r$.

We believe that the relation between these two variables is as follows. As shown in the paragraph about the stability of the axisymmetric sand bed, the azimuthal fluid motion transports glass spheres along the sand bed. The action of the Coriolis force $f_c \sim \rho_l U \Omega_r$ on the azimuthal component of fluid velocity U induces the appearance of a vortical fluid flow of radius L. The centrifugal acceleration of this circular motion is scaled as U^2/L. The fluid transports glass spheres along the sand bed and thereby imposes the wavelength $\lambda = \lambda(L)$. Using a typical value of fluid velocity $U \equiv b\Omega_{\rm osc}$, we can estimate the size of the ripples:

$$\lambda \sim b\Omega_{\rm osc}/\Omega_r. \tag{6}$$

According to Eq. (6), the typical length along the interface between the fluid and the sand bed is not the amplitude of fluid oscillation b but the distance $b^* \equiv b\Omega_{\rm osc}/\Omega_r$, which is the displacement distance of liquid during a rotation cycle.

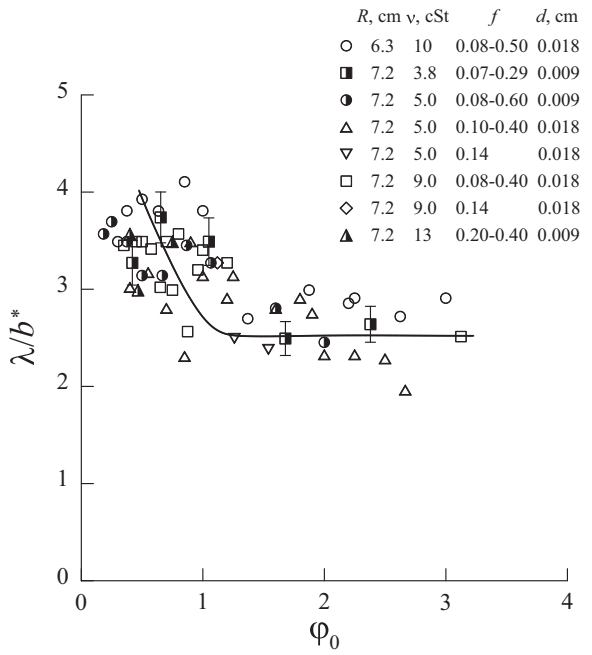

FIG. 9. Nondimensional wavelength of the dunes versus the angular amplitude of oscillation.

Figure 9 shows the dependence of the nondimensional azimuthal length λ/b^* of the dunes on the angular amplitude of oscillation φ_0. It is noteworthy that the experimental data are satisfactorily consistent for different viscosities and particle sizes. In the range $\varphi_0 > 1$, the ratio λ/b^* is nearly constant and approximately equal to 2.5. This result is consistent with the reported data by [12,14,15,25].

C. Ripples migration

Figure 10 demonstrates the time evolution of dunes in the course of a long-term experiment: symbols illustrate the positions of the dune crests. With time, the number of dunes decreases because of coalescence: small dunes bump into larger ones. A few minutes later, the number of dunes reaches a quasisteady value. According to the observations, the dunes migrate in the azimuthal direction. At first sight, this result is puzzling because the liquid undergoes pure oscillatory flow.

We offer the following explanation for this intriguing phenomenon. In a rotating and oscillating cylinder, the liquid bulk rotates as a solid body at a constant rotation rate Ω_r almost everywhere except the thin viscous boundary layers near the sand surface and end walls of a cylinder. Because the angular velocity Ω oscillates around the mean rotation rate Ω_r [see Eq. (1)], the liquid rotates more slowly than the cylinder during the first half cycle of oscillation and faster than the cylinder during the second half cycle. Moreover, in the cylinder's frame of reference, the directions of azimuthal liquid flow in the first and second half cycles are the opposite. During the first half cycle, the liquid flow transports sand grains in the direction opposite to the cylinder's rotation (so-called backward migration). During the second half cycle, sand grains are transported in the direction of the cylinder's rotation

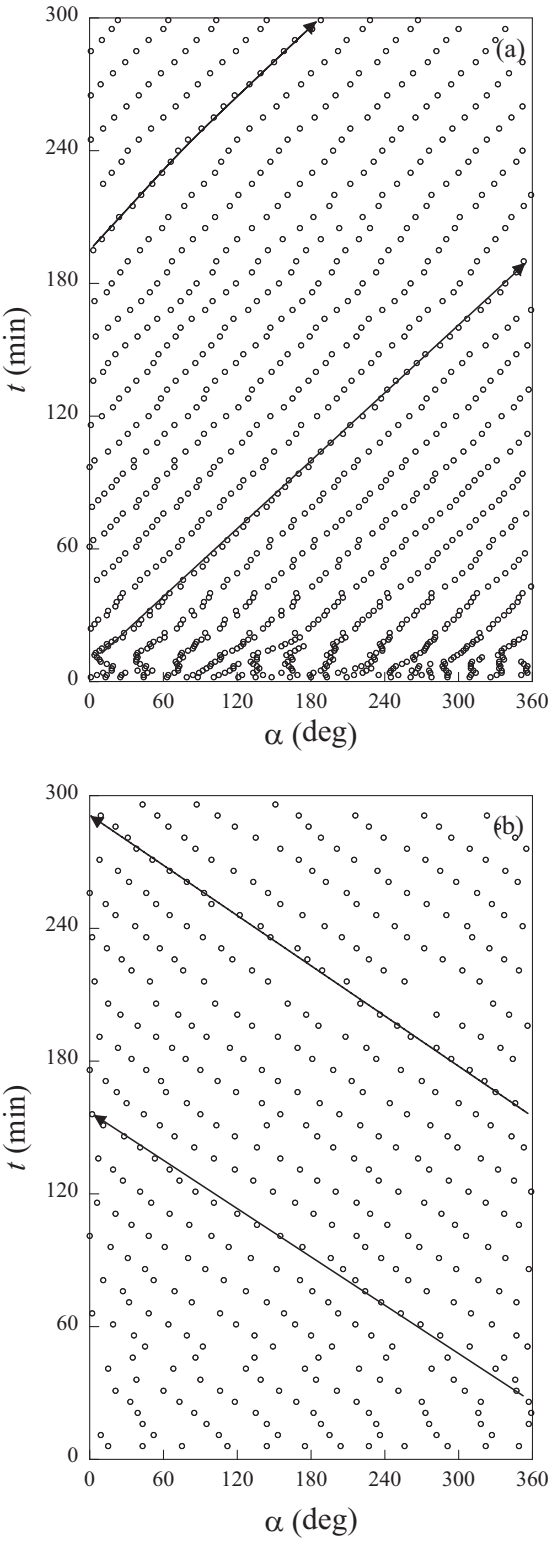

FIG. 10. Spatiotemporal evolution of dunes: $R = 6.3$ cm, $h_0 = 0.45$ cm, $\nu = 10$ cSt, $d = 0.018$ cm, $\Omega_r = 31.4$ rad/s, $\Omega_{\rm osc} = 12.6$ s^{-1}, $\epsilon = 0.17$ (a) and 0.22 (b); the symbols illustrate the positions of the dune crests. The azimuthal angle α increases in the direction of the cylinder rotation.

(forward migration). One can imagine that the total mass flux is zero, but it is not because of the unequal action of centrifugal

force on the sand granules in the first and second half cycles of oscillation. During the first half cycle, when the cylinder rotates faster than the liquid interior, the granules experience a larger centrifugal force and travel backward a shorter distance. During the second half cycle, the centrifugal force decreases and the granules travel forward a longer distance. Therefore, the total mass transport is codirected with the cylinder rotation [Fig. 10(a)].

The typical velocity Ω_{drift} of this mass transport is on the order of a few degrees per minute [Fig. 10(a)]. The velocity of migration remains constant because the number of dunes reaches the steady-state value.

Surprisingly, the direction of mass transport can reverse at a large amplitude of oscillation [Fig. 10(b)]. An intuitive explanation of the backward migration is as follows. When the amplitude of oscillation is relatively small, sand is dragged by the liquid flow along the windward side; after reaching the dune crest, it is redistributed along the slip face. During the following half cycle, the process is repeated in the opposite direction. As previously discussed, this phenomenon leads to the onset of forward migration. What will change at larger amplitudes? According to the observations, the transition from the vortex ripple flow to the sheet flow occurs [Figs. 7(e) and 7(f)]. During the half cycle, when $\Omega < \Omega_r$ (i.e., under reduced centrifugal force), the granules are transported in the direction of the cylinder rotation and obtain a sufficiently large velocity to become suspended in the liquid. During the following half cycle (under increased centrifugal force), the granules deposit on the interface, whereas the sediment cloud is transported in the backward direction.

Backward migration of dunes is a rare but not unique phenomenon. In laboratory experiments, Dumas *et al.* [9] observed similar dynamics of subaqueous sand dunes generated under combined flows. However, the relevant dynamical mechanism that controls the backward migration of sand dunes remains unclear. Dumas *et al.* [9] noted that the phenomenon of backward migration only appeared in the intensive oscillatory flow. This fact is qualitatively consistent with our experimental data: In a rotating and oscillating cylinder, the effect of backward migration appears at large oscillation acceleration amplitude $b\Omega_{\text{osc}}^2$, i.e., intensive liquid oscillation (negative drift velocity Ω_{drift} in Fig. 11). Experimental data analysis shows that the region of existence of forward migration narrows when the nondimensional frequency f increases. We observe an exclusively forward drift at $f = 0.20$, an exclusively backward drift at $f = 0.50$, and both types of dune migration at intermediate values of f.

Figure 12 demonstrates the dependence of the nondimensional drift velocity on the ratio between wavelength λ and amplitude of oscillation b. The experimental data points tend to fall on a single curve if they are obtained at close values of f but various values of the mean rotation rate Ω_r and frequency of oscillation Ω_{osc} (triangles in Fig. 12). This result proves that the nondimensional frequency f is one of the parameters that controls the dune migration.

We expect that at smaller values of λ/b, the drift velocity of the dunes at $f = 0.20$ (squares in Fig. 12) decreases; in fact, all curves have similar shapes regardless of f. With the increase in ϵ, the curves shift to the right (larger values of λ/b) and the domain of existence of the forward migration narrows.

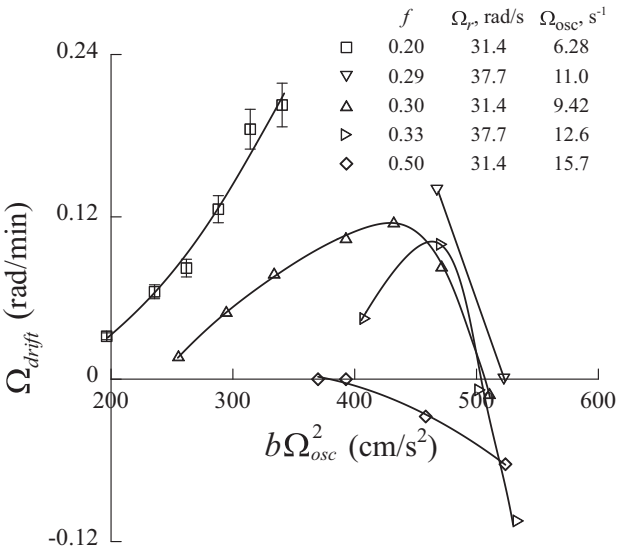

FIG. 11. Dependence of the drift velocity on the amplitude of the tangential acceleration of the cylinder. The experiments were performed with particles with mean diameter $d = 0.018$ cm: $R = 7.2$ cm, $\nu = 10$ cSt.

This figure shows that the dependence of the drift velocity on the ratio between wavelength λ and amplitude of oscillation b is nonmonotonic. According to the analysis of dune migration, this effect can be explained by the transition from the regime of vortex ripples to the sheet flow. In the vortex ripple regime, dunes migrate in the direction of the cylinder rotation: The positive drift velocity decreases with the increase in nondimensional length λ/b (the right side of the curves in Fig. 12). The transition to the sheet flow leads to the reverse of the direction of dune migration (the left side of the curves in Fig. 12).

By combining two control parameters $f = \Omega_{\text{osc}}/\Omega_r$ and λ/b, we introduce a new parameter λ/b^* to accommodate

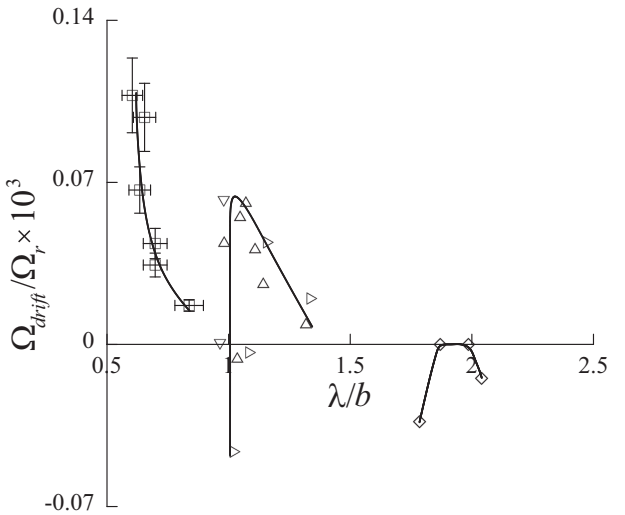

FIG. 12. Dependence of the nondimensional drift velocity on the nondimensional wavelength λ/b. The symbols correspond to those in Fig. 11.

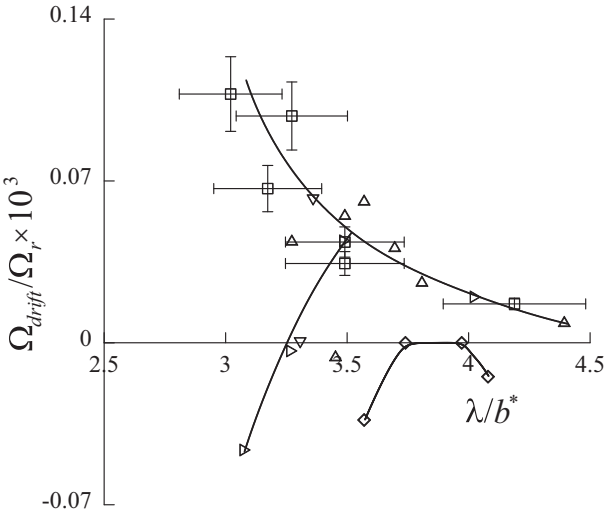

FIG. 13. Dependence of the nondimensional migration velocity on the ratio between wavelength λ and distance b^*. The symbols correspond to those in Fig. 11.

various data on the drift velocity. Here, $b^* \equiv b\Omega_{\rm osc}/\Omega_r$ is the displacement distance of liquid during a rotation cycle. As we have identified, λ/b^* determines the size of the dunes in the range of large cylinder oscillation amplitudes (see Fig. 9). Figure 13 illustrates that the experimental results obtained at different values of f are consistent with one another, but only in the vortex ripple regime, wherein the drift velocity decreases with the increase in nondimensional length λ/b^*. Thus, the displacement distance of liquid during a rotation cycle controls the velocity of forward migration in the vortex ripple regime (the right side of the curves in Figs. 12 and 13). The appearance of the left side of the curves can be explained by the transition to the sheet flow. In the framework of this discussion, the data on the backward migration rate are not clearly understood and require further investigation. We believe that more advanced analysis will determine the relevant dynamical mechanism that controls the forward and backward dune migration.

IV. CONCLUSION

The dynamics of granular medium in a liquid-filled horizontal cylinder with a time-varying rotation rate was experimentally studied. When the cylinder purely rotates, the granular medium develops an annular layer near the cylindrical wall and undergoes a solid-body rotation. The interface between fluid and sand is smooth and axisymmetric. The time variation of the rotation rate initiates the azimuthal oscillation of liquid in the cylinder's frame of reference and provokes regular ripple formation. According to the analysis, the ripples grow if there is a quasisteady instability of oscillatory liquid motion. In the range $\mathrm{Re}_\delta > 100$, the threshold of ripple formation is determined by a critical Shields number $\theta_c \simeq 0.05$.

The spatial period of the relief is based on the displacement distance of fluid during a rotation cycle $b^* = b\Omega_{\rm osc}/\Omega_r$ and is not sensitive to the fluid viscosity and granule size. This result demonstrates the fundamental difference between ripples formed in the rotating containers and those formed in the nonrotating ones, where the ripple length is determined by the amplitude of fluid oscillation.

The experimental data which were obtained in cylinders of different radii with granules of various diameters, obey the law $\lambda/b^* \simeq 2.5$ in the range of large cylinder oscillation amplitudes $\varphi_0 > 1$. In long-term experiments, we observed dune migration in the direction of rotation of the cylinder or the opposite direction. Forward migration is observed in the vortex ripple regime and can be explained by the asymmetric action of the centrifugal force on the granules in opposite phases of an oscillation cycle. The forward migration rate is determined by the nondimensional wavelength and decreases with λ/b^*. The backward migration occurs in the sheet-flow regime. The mechanism responsible for the observed backward migration is not clearly understood and requires further investigation.

ACKNOWLEDGMENTS

The work is supported by Grant No. 14-11-00476 of the Russian Science Foundation.

[1] G. G. Stokes, Trans. Cambridge Philos. Soc. **8**, 441 (1847).
[2] P. Blondeaux, E. Foti, and G. Vittori, Eur. J. Mech. B: Fluids **19**, 285 (2000).
[3] C. Faraci and E. Foti, Phys. Fluids **13**, 1624 (2001).
[4] R. W. G. Carter, *Coastal Environments: An Introduction to the Physical, Ecological, and Cultural Systems of Coastlines* (Elsevier, New York, 2013).
[5] R. A. Bagnold and G. Taylor, Proc. R. Soc. London, Ser. A **187**, 1 (1946).
[6] M. Scherer, F. Melo, and M. Marder, Phys. Fluids **11**, 58 (1999).
[7] J. S. Ribberink, J. J. van der Werf, and T. O'Donoghue, in *Particle-Laden Flow* (Springer, New York, 2007), pp. 3–14.
[8] F. Charru, B. Andreotti, and P. Claudin, Annu. Rev. Fluid Mech. **45**, 469 (2013).
[9] S. Dumas, R. Arnott, and J. B. Southard, J. Sediment. Res. **75**, 501 (2005).
[10] J. R. Lacy, D. M. Rubin, H. Ikeda, K. Mokudai, and D. M. Hanes, J. Geophys. Res.: Oceans **112**, (2007).
[11] J. P. Davis, D. J. Walker, M. Townsend, and I. R. Young, J. Geophys. Res.: Oceans **109**, (2004).
[12] A. Ivanova and V. Kozlov, Fluid Dyn. **37**, 277 (2002).
[13] G. Rousseaux, H. Caps, and J.-E. Wesfreid, Eur. Phys. J. E **13**, 213 (2004).
[14] G. Rousseaux, J. Kruithof, P. Jenffer, and J. E. Wesfreid, Phys. Rev. E **78**, 016302 (2008).
[15] A. Stegner and J. E. Wesfreid, Phys. Rev. E **60**, R3487 (1999).
[16] V. Dyakova, V. Kozlov, and D. Polezhaev, Shock Vibr. **2014**, 841320 (2014).
[17] X. Wu, P. Bender, S. Peale, G. Rosborough, and M. Vincent, Planet. Space Sci. **45**, 15 (1997).

[18] S. J. Peale, R. J. Phillips, S. C. Solomon, D. E. Smith, and M. T. Zuber, Meteorit. Planet. Sci. **37**, 1269 (2002).
[19] J.-L. Margot, S. Peale, R. Jurgens, M. Slade, and I. Holin, Science **316**, 710 (2007).
[20] T. Van Hoolst, N. Rambaux, Ö. Karatekin, V. Dehant, and A. Rivoldini, Icarus **195**, 386 (2008).
[21] P. Nielsen, *Coastal Bottom Boundary Layers and Sediment Transport* (World Scientific, Singapore, 1992), Vol. 4.
[22] C. Von Kerczek and S. H. Davis, J. Fluid Mech. **62**, 753 (1974).
[23] V. Kozlov, Fluid Dyn. **14**, 904 (1979).
[24] V. Kozlov and D. Polezhaev, Phys. Rev. E **92**, 013016 (2015).
[25] R. A. Bagnold, *The Physics of Blown Sand and Desert Dunes* (Courier Corporation, North Chelmsford, MA, 2012).